ACS OMEGA

http://pubs.acs.org/journal/acsodf
Article

CO Oxidation at Low Temperatures over the Au Cluster Supported on Crystalline Silicotitanate

Miyu Muraoka, Takuto Miyatani, Akihiro Sembuku, Tamao Ishida, Toru Murayama, Yoshihiro Kubota, and Satoshi Inagaki*

Cite This: *ACS Omega* 2024, 9, 41696−41702

Read Online

ACCESS | Metrics & More | Article Recommendations | Supporting Information

ABSTRACT: Crystalline silicotitanate (CST) with a sitinakite structure has attracted considerable attention as an ion exchanger because of its anionic surface owing to SiO_4 tetrahedral and TiO_6 octahedral linked structures. In particular, the anionic surface of CST is advantageous in immobilizing single Au atoms derived from a cationic precursor such as $Au(en)_2Cl_3$ (en = ethylenediamine). In this study, a Au/CST catalyst was prepared and evaluated for CO oxidation. The transmission electron microscopy and X-ray photoelectron spectroscopy results suggest that Au single atoms and clusters ($Au^{\delta+}$, $0 < \delta < 1$) were supported on Na^+−CST particles. The 1.0 wt % Au/CST catalyst yielded high catalytic activity for CO oxidation, where 50% CO oxidation was achieved at a low temperature of −13 °C. In the low-temperature region (from −84 to 20 °C), CO oxidation over Au/CST may progress through the well-known Langmuir−Hinshelwood mechanism. Conversely, the experimental results of CO oxidation without O_2 confirmed that the reaction proceeded according to the Au-assisted Mars−van Krevelen mechanism using the lattice oxygens of the CST particles at temperatures above 20 °C. Therefore, this work contributes to the design of highly dispersed single-atom or cluster catalysts using the anionic surface of the microporous CST.

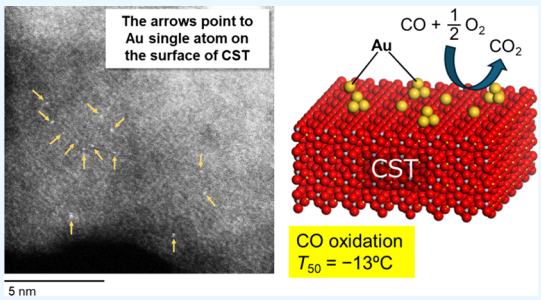

1. INTRODUCTION

Crystalline microporous materials, such as zeolites, metal−organic frameworks, and covalent organic frameworks, are good catalysts, adsorbents, and separation membranes because their ordered micropores with large surface areas can diffuse reactants and provide efficient reaction fields. Zeolite frameworks and related inorganic porous materials are negatively charged because some Si^{4+} ions are isomorphically substituted with Al^{3+}. As such, cations exist on the material surface and are reversibly exchangeable with other cations through liquid-phase treatment to maintain a neutral charge.

Poojary et al. reported the hydrothermal synthesis of sodium titanosilicate with an ideal composition of $Na_2Ti_2O_3SiO_4 \cdot 2H_2O$ in highly alkaline media with its crystalline structure solved using X-ray diffraction (XRD) data as a structural analogue of sitinakite.[1] The resulting material is a crystalline silicotitanate (CST), which has regularly combined cubane-like Ti_4O_4 units and SiO_4 tetrahedra, resulting in rigid and uniform three-dimensional microporous structures, such as zeolites (Figure 1).[1,2] Hexacoordinated Ti^{4+} and tetracoordinated Si^{4+} are bonded via an oxygen atom, and a countercation is placed on the microporous surface to compensate for the negative charge delocalized on the framework oxygen atoms. Moreover, H^+−CST can be prepared by ion exchange via acid treatment.[3] As such, CST is used as an industrial adsorbent of radioactive elements owing to its highly selective ion exchange with $^{90}Sr^{2+}$ and $^{137}Cs^+$.[3,4] Various microporous crystals contain Si and Ti atoms, which are useful for selective oxidation reactions as solid catalysts. Among these, TS-1 is a titanosilicate (typically, Si/Ti > 45) with an MFI structure with the regular combination of SiO_4 and TiO_4 tetrahedra and an electrically neutral surface. Meanwhile, microporous silicotitanates, such as CST (Si/Ti = 0.50),[1,2] as well as GTS-1 (Si/Ti = 0.75)[4] and ETS-10 (Si/Ti = 5.00),[4] have anionic surfaces because of their SiO_4 tetrahedral and TiO_6 octahedral linked structures, where one SiO_4 tetrahedron is adjacent to one TiO_6 octahedron. These silicotitanates are mainly utilized as ion exchangers,[3,4] not as solid catalysts. However, the anionic surface of CST and related materials has a great advantage in the immobilization of single atoms, such as Au, Pt, and Ir, via ion-exchange treatment or impregnation of cationic precursors, yielding highly active catalysts for oxidation and reduction reactions.[5−8] Specifically, the control of the hydrothermal synthesis conditions can obtain small CST particles (less than 50 nm),[9] which are useful in dispersing single-atom Au species on the surface.

Received: June 20, 2024
Revised: August 5, 2024
Accepted: August 30, 2024
Published: September 26, 2024

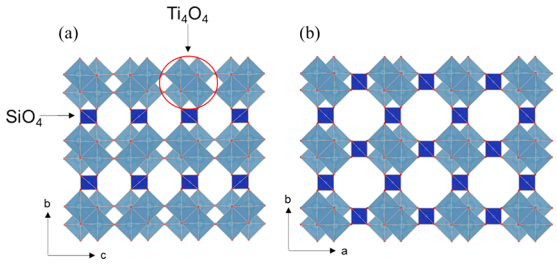

Figure 1. Framework models of CST with a sitinakite structure. View along the (a) [100] direction and (b) [001] direction.

Au had been considered as a catalytically inert element for a long time until the high catalytic activity of Au-supporting catalysts for CO oxidation at low temperatures (−70 °C)[10,11] and catalytic activity of the Au chloride catalyst for hydrochlorination of acetylene[12,13] were reported by Haruta et al. and Hutchings et al., respectively. CO oxidation often serves as a prototypical heterogeneously catalyzed reaction using Au catalysts supported on various metal oxides.[14] In this reaction, the size of the Au nanoparticles (NPs, <5 nm) and O_2 activation at the perimeter interface between the Au NPs and metal oxides are considered important factors for high catalytic activities.[15−19] The electrostatic interaction between the anionic surface of the CST crystals and the cationic Au source, $[Au(en)_2]^{3+}$ (en = ethylenediamine), is expected to immobilize atomic Au species on the catalyst support to achieve high catalytic activity, even at low temperatures (less than 0 °C).

In the early stages of research, Au/Fe_2O_3, Au/Co_3O_4, and Au/NiO were prepared by the coprecipitation (CP) technique using metal nitrates.[10,11] Deposition−precipitation (DP) was eventually developed to apply MO_x species (e.g., TiO_2, Ta_2O_5, and Nb_2O_5) that cannot be prepared by CP because there are no metal nitrates.[20−24] However, the deposition of Au NPs on acidic supports, such as Ta_2O_5 and Nb_2O_5, using the conventional DP method is difficult[22,23] because negatively charged Au precursors, such as $[AuCl(OH)_3]^-$ or $[Au(OH)_4]^-$, electrostatically repulse their negatively charged surface in aqueous solutions with over a wide range of pH values. Therefore, the sol immobilization (SI) technique using Au nanocolloids stabilized by 1-dodecanethiolate has been applied to acidic supports.[25] Another approach for the deposition of Au NPs on acidic supports is the deposition−reduction method using $[Au(en)_2]Cl_3$ and $NaBH_4$ as the precursor and reducing agent, respectively.[26−28] Other preparation methods, including DP using $[Au(en)_2]Cl_3$ as the precursor, DP-urea,[29,30] solid grinding,[31,32] and impregnation using halide-free Au−amino acid complexes as precursors,[33] have been developed to deposit Au NPs and clusters onto almost all types of supports, including acidic oxides, nonoxides, carbons, and polymers.

In this study, 1.0 wt % Au/CST was prepared by the DP method using $Au(en)_2Cl_3$, designated as Au(DP)/CST, because the anionic surface of CST led to a high dispersion of cationic $[Au(en)_2]^{3+}$ species, resulting in the formation of Au clusters as highly efficient catalytic active sites for CO oxidation with O_2 at ambient temperature. The physicochemical states of Au on the CST crystals were characterized by using XPS and TEM observations, and the Au(DP)/CST and the related catalysts were evaluated for CO oxidation. Furthermore, a possible reaction mechanism for CO oxidation over the Au(DP)/CST catalyst was studied by evaluating the activation energy and observing CO reaction without O_2 using temperature-programmed reaction measurements.

2. EXPERIMENTAL SECTION

2.1. Preparation of Na^+−CST. Na^+−CST crystals were synthesized following a typical synthesis procedure.[9] Tetraisopropyl orthotitanate ($Ti(OC_3H_7)_4$, TCI; 2.4925 g, 8.77 mol-Ti) was added to aqueous NaOH solution (8 mol L^{-1}, 6.353 mmol g^{-1}, Wako Chemicals; 22.9813 g, 146.0 mmol NaOH) in a 180 mL Teflon beaker under gentle stirring. Tetraethyl orthosilicate ($Si(OC_2H_5)_4$, Wako Chemicals; 4.2083 g, 20.2 mmol-Si) was added to the mixture and stirred for 30 min. Subsequently, distilled water (35.028 g, 1944 mmol) was added and stirred for 30 min. The molar composition of the resulting mixture was 1.0 TiO_2:2.27 SiO_2:16.4 NaOH:327 H_2O. The obtained white suspension was transferred into a 125-mL Teflon-lined stainless-steel autoclave and subjected to hydrothermal synthesis at 180 °C for 48 h in a convection oven. After crystallization, the mixture was filtered, rinsed with distilled water, and dried in an oven at 80 °C overnight to obtain a white powder (1.2792 g).

2.2. Preparation of Au(DP)/CST. Au(DP)/CST was prepared by the DP method using $Au(en)_2Cl_3$ as the Au precursor. For the preparation of 1.0 wt % Au(DP)/CST, a hydrogen tetrachloroaurate aqueous solution ($HAuCl_4$, 2.54 mol L^{-1}; 0.590 mL, 1.5 mmol of Au) was mixed with diethyl ether (5.0 mL). Meanwhile, ethylenediamine (0.30 mL) was separately diluted in diethyl ether (2.0 mL). Subsequently, a yellow precipitate was formed after adding the ethylenediamine solution to the Au solution in a glass beaker. The mixture was heated in a water bath at 75 °C to dissolve the precipitates. An appropriate amount of distilled water was added dropwise until the precipitate was completely dissolved. After ethanol droplets were added, the solution was cooled overnight in a refrigerator to obtain $Au(en)_2Cl_3$ crystals. After complete precipitation, a yellow crystalline powder (0.2802 g) was recovered by filtration, rinsing with ethanol, and drying *in vacuo* at 40 °C overnight. After the obtained $Au(en)_2Cl_3$ powder (21.5 mg) was dissolved in distilled water (40 mL), Na^+−CST (1.0 g) was added to the Au solution and stirred gently at 70 °C for 60 min. Subsequently, the mixture was centrifuged at 3200 rpm for 10 min for five cycles. The precipitate was dried in an oven at 80 °C overnight. The recovered powder was heated in a muffle furnace in air at a ramping rate of 1.5 °C min^{-1} and maintained at 300 °C for 4 h. The calcined Au(DP)/CST sample has 1.0 wt % Au.

For the preparation of 0.3 wt % Au(DP)/CST, hydrogen tetrachloroaurate tetrahydrate (99.9%, Wako Chemicals; 0.5052 g, 1.21 mmol-Au) was dissolved in distilled water (5.0308 g). Ethylenediamine (0.215 mL) was added to the yellow solution, and the mixture turned brown. The mixture was stirred gently at room temperature for 30 min. When ethanol (30 mL) was added dropwise to the mixture with gentle stirring, a yellowish precipitate was gradually formed. The yellow $Au(en)_2Cl_3$ powder (0.4347 g) was recovered by filtration, rinsing with ethanol, and drying *in vacuo* at room temperature for 5 h.

After the obtained $Au(en)_2Cl_3$ powder (10.4 mg) was dissolved in distilled water (70 mL), Na^+−CST (1.5 g) was added to the Au solution, and the mixture was stirred gently at 70 °C for 60 min. The mixture was then centrifuged thrice at 3300 rpm for 5 min. The precipitate was dried overnight at 80

https://doi.org/10.1021/acsomega.4c05778
ACS Omega 2024, 9, 41696−41702

°C in an oven. The recovered powder was heated in a muffle furnace in air at a ramping rate of 1.5 °C min^{-1} and maintained at 300 °C for 4 h. The Au content of the calcined Au(DP)/CST sample was 0.30 wt %.

2.3. Preparation of Au(SI)/CST. The SI technique using Au nanocolloids (~3 nm) stabilized by 1-dodecanethiolate was used to prepare the Au/CST catalyst as the reference; the obtained sample was designated as Au(SI)/CST. Na^+−CST (1.0 g) was suspended in toluene (40 mL). Meanwhile, Au−S colloids (Tanaka Precious Metals; 13.6 mg) were suspended in toluene (10 mL). The colloidal solution was added dropwise to the Na^+−CST suspension with gentle stirring. The mixture was continuously stirred at room temperature for 60 min. The solvent was removed from the mixture using a rotary evaporator, and a solid residue was recovered and dried *in vacuo* at room temperature overnight. The recovered solid was then calcined by using the aforementioned procedure. Calcined Au(SI)/CST has 1.0 wt % Au.

2.4. Characterization. The crystallinity of the CST samples prepared in this study was analyzed by powder XRD using an Ultima-IV diffractometer (Rigaku) with Cu Kα radiation at 40 kV and 20 mA. The specific surface area of the Na^+−CST sample was calculated based on multipoint N_2 adsorption−desorption data acquired using a gas sorption analyzer (BELSORP-MaxII, MicrotracBEL Corp.) at −196 °C. The samples were heated *in vacuo* (<1 Pa) to 100 °C for more than 12 h prior to measurement. The specific surface area was obtained from the adsorption isotherm using the Brunauer−Emmett−Teller (BET) equation. The particle size and shape of the CST samples were observed using semi-in-lens-type field-emission scanning electron microscopes (FE-SEM, SU8010 and SU8600 Regulus Series, Hitachi High-Tech) equipped with a cold-field emitter as an electron source. High-resolution images were taken at accelerating voltages of 0.7 and 1.0 kV by applying a beam deceleration technique. High-angle annular dark-field scanning transmission electron microscopy (HAADF-STEM) was performed using a JEM-ARM200F NEOARM (JEOL) and Titan Cubed G2 60-300 (FEI) microscope to obtain the particle-size distribution of Au supported on the CST. The Au content of the samples was measured using inductively coupled plasma atomic emission spectrometry (ICPE-9000, Shimadzu Corp.). The oxidation state of the Au species was characterized by X-ray photoelectron spectroscopy (XPS; QuanteraSXM, ULVAC-Phi) using Al Kα radiation with 300 scans at a pass energy of 69 eV.

The temperature-programmed CO oxidation without gaseous O_2 over the Au/CST catalyst was performed by using a BELCAT-II catalyst analyzer (MicrotracBel) equipped with a mass spectrometer. The Au/CST sample was preheated to 250 °C for 30 min under Ar flow (30 cm^3 min^{-1}) and then cooled to −100 °C. After changing to 30 cm^3 min^{-1} He and maintaining it for 30 min, the CO oxidation reaction was carried out under 0.5% CO/He flow (30 cm^3 min^{-1}) at a ramping rate of 10 °C min^{-1} up to 200 °C. Subsequently, the treated sample was preheated to 250 °C for 30 min under 20% O_2/Ar flow (30 cm^3 min^{-1}) and then cooled to −100 °C under the same gas flow. After He flushing for 30 min, the CO oxidation was performed according to the aforementioned procedure. During CO oxidation, CO_2 was continuously detected as a fragment of m/z = 44.

2.5. Catalytic Activity Test of Au/CST. CO oxidation was performed in a U-shaped glass fixed-bed flow reactor. The catalyst (150 mg) was pretreated with 20% O_2/N_2 (50 cm^3 min^{-1}) at 250 °C for 60 min. The reactant gas (1 vol % CO in air) was passed through the catalyst at 50 cm^3 min^{-1}. The space velocity was 20,000 cm^3 h^{-1} (g-catalyst)$^{-1}$. The reaction temperature was varied from −84 to 153 °C. The compositions of the inlet and outlet gases were determined by using an online 490 micro-GC system (Agilent Technologies). The turnover frequency (TOF) based on the total number of Au atoms at 22 °C was calculated by adjusting the amount of catalyst to maintain the CO conversion to less than 15%. The reaction rates were measured to calculate the activation energy (E_a) and reaction orders with a CO conversion of less than 20% by varying the catalyst weight. The reaction order of CO was measured with 0.4−1.0 vol % CO and 20 vol % O_2. The reaction order of O_2 was also measured with 2−30 vol % O_2 and 1.0 vol % CO.

3. RESULTS AND DISCUSSION

3.1. Synthesis and Characterization of Au/CST. The XRD pattern of the compound synthesized in this study (Figure 2b) corresponds well with the simulated XRD pattern of the sitinakite structure (Figure 2a), indicating the successful crystallization of Na^+−CST without any impurities. The high-resolution FE-SEM images (Figure S1a,b) showed that Na^+−CST with small particle sizes of 50−80 nm was obtained, and the shape was almost cuboid, which is consistent with the tetragonal space group, $P4_2/mcm$, for the sitinakite structure.[1,2] This sample has a specific surface area of approximately 73 m^2 g^{-1}, estimated from the nitrogen adsorption isotherm (Figure S1c). The Au NPs supported on Na^+−CST were prepared by the DP method using $Au(en)_2Cl_3$, designated Au(DP)/CST, and the SI method using Au−S colloids (Au(SI)/CST). The as-prepared samples were calcined at 300 °C to remove the

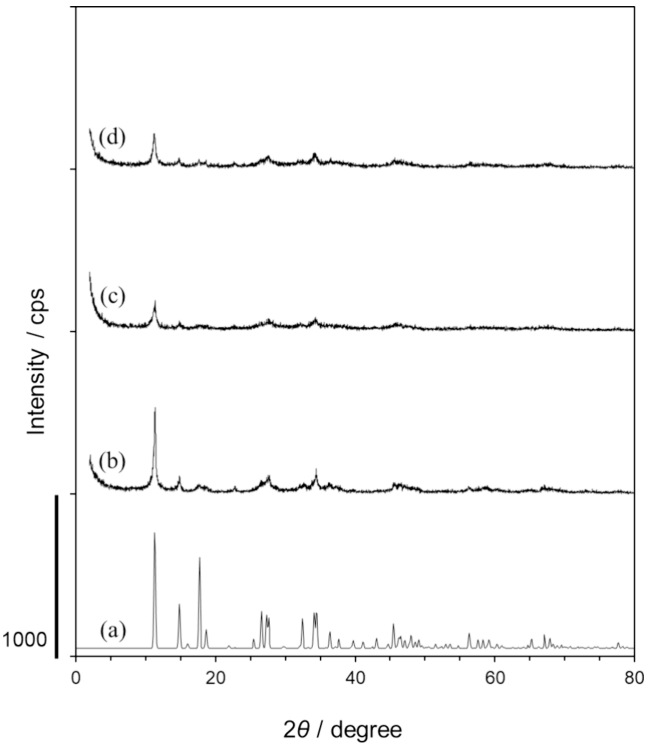

Figure 2. (a) Simulated XRD pattern of the sitinakite structure[2] and XRD patterns of (b) Na^+−CST, (c) 1.0 wt % Au(DP)/CST, and (d) 1.0 wt % Au(SI)/CST.

https://doi.org/10.1021/acsomega.4c05778
ACS Omega 2024, 9, 41696−41702

ligands and form Au^0 NPs. The XRD patterns of 1.0 wt % Au(DP)/CST and 1.0 wt % Au(SI)/CST (Figure 2c and Figure 2d, respectively) indicate the retained sitinakite structure after calcination, and XRD peaks corresponding to Au metal crystals were not observed. This denotes the extremely small size of the Au species supported on the CST particles. The Au particle-size distribution was determined by TEM (Figure S2a,b). The estimated average particle size of Au in Au(DP)/CST was 3.1 ± 1.2 nm, and that of Au(SI)/CST was 3.2 ± 1.0 nm. Unfortunately, Au particles less than 1 nm were not observed in the TEM images at lower magnification. In the high-resolution TEM images at a higher magnification, single Au atoms and clusters (less than 1 nm in size) were observed in Au(DP)/CST (Figure 3a), whereas Au NPs smaller than 1 nm were not observed in Au(SI)/CST (Figure 3b). This is attributed to the high dispersion of the cationic Au precursor on the anionic surface of the CST to yield single Au atoms and clusters in Au(DP)/CST.

The electronic states of Au were evaluated from the XPS profiles of Au(DP)/CST, Au(SI)/CST, and Au/TiO_2 (Figure 4). For the Au 4f core-level region, the peaks (83.0−83.3 and 86.6−86.9 eV) of Au^0 were obtained from all samples at almost the same positions.[34] Notably, Au(DP)/CST showed distinct peaks at 84.88 and 88.56 eV (Figure 4a), corresponding to $Au^{\delta+}$ species,[35] probably because $Au^{\delta+}$ can be stabilized on the anionic surface of CST particles. It is speculated that such $Au^{\delta+}$ species may be incorporated into a part of the peripheral sites of the Au clusters on the CST surface, resulting in a strong interaction between the Au clusters and the CST, thus avoiding sintering during the CO oxidation. Namely, the TEM and XPS results reveal that Au clusters (<1 nm) can be successfully formed on the CST particles during the Au-$(en)_2Cl_3$ deposition followed by calcination.

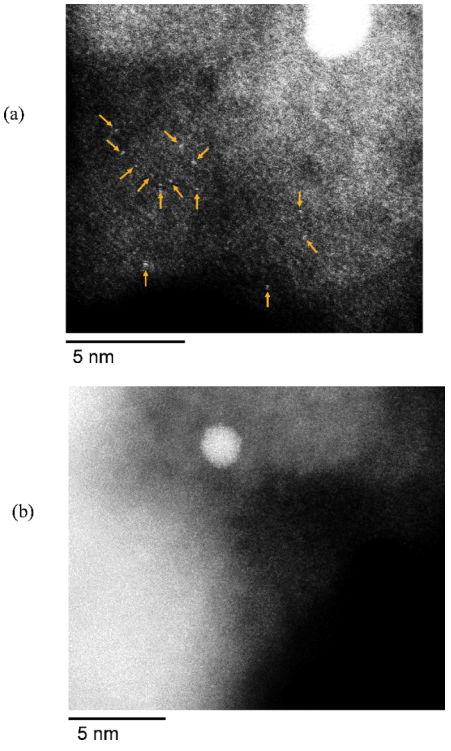

Figure 3. High-resolution TEM images of (a) 1.0 wt % Au(DP)/CST and (b) 1.0 wt % Au(SI)/CST. The arrows in panel (a) point to Au single atoms and/or clusters.

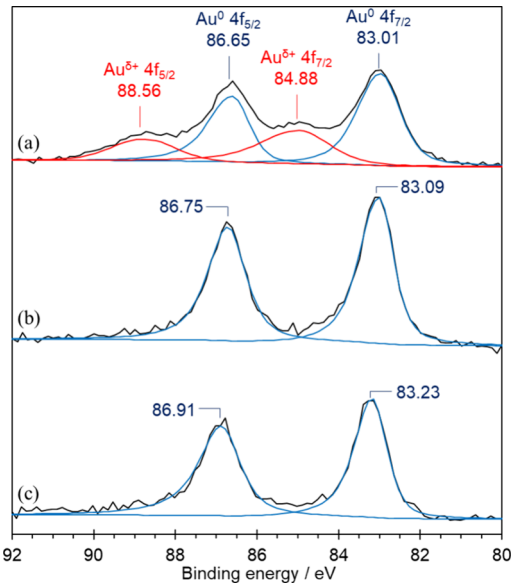

Figure 4. Au $4f_{5/2}$ and Au $4f_{7/2}$ spectra of XPS for (a) 1.0 wt % Au(DP)/CST, (b) 1.0 wt % Au(SI)/CST, and (c) 1.0 wt % Au/TiO_2.

3.2. Catalytic Activity of Au/CST for CO Oxidation.

The catalytic oxidation reaction of CO with O_2 was carried out from −84 to 153 °C to determine the temperatures for 50% CO conversion (T_{50}) of Au(DP)/CST and Au(SI)/CST with 1.0 wt % Au (Figure 5). The 1.0 wt % Au(DP)/CST showed sufficient catalytic activity even at extremely low temperatures of −84 °C, and the CO conversion gradually increased up to 91.0% at 25 °C. The T_{50} of the catalyst was estimated at −13 °C. A conventional catalyst, that is, 1.0 wt % Au/TiO_2 (Au size, 4.1 ± 1.1 nm),[23] efficiently operates for this oxidation reaction with a T_{50} of 21 °C. These results indicate that Au(DP)/CST has a high potential for CO oxidation. The CO oxidation over 1.0 wt % Au(SI)/CST (Au size, ∼3 nm) was observed with a T_{50} of 38 °C. The higher catalytic activity of Au(DP)/CST than that of Au(SI)/CST suggests that more dispersed Au species (size of <1 nm) exert highly efficient catalytic activity for CO oxidation in the low-temperature range of −100 to 25 °C.

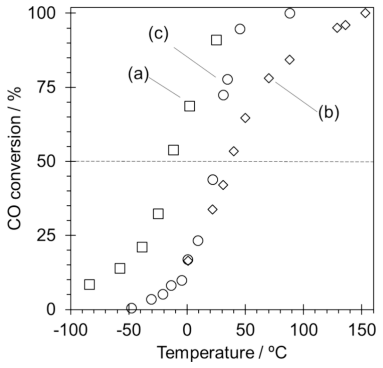

Figure 5. Effect of the reaction temperature on CO oxidation with O_2 over (a) 1.0 wt % Au(DP)/CST, (b) 1.0 wt % Au(SI)/CST, and (c) 1.0 wt % Au/TiO_2. Reaction conditions: weight of the catalyst, 150 mg; 1% CO/air (50 cm^3 min^{-1}).

https://doi.org/10.1021/acsomega.4c05778
ACS Omega 2024, 9, 41696−41702

After the reaction temperature was varied from −84 to 153 °C, both the spent Au(DP)/CST and Au(SI)/CST maintained the catalytic activity at the original level. In TEM observation (Figure S2), the distribution of the Au particle size for the Au(DP)/CST remained unchanged after the CO oxidation under robust conditions. Notably, a large number of very small Au clusters (size <1 nm) were observed in the spent catalyst in the high-magnification TEM images (Figure S3). Moreover, the Au-XPS profile of the spent Au(DP)/CST was very similar to that of the pristine Au(DP)/CST (Figure S4a,b). These results reveal that the highly dispersed Au clusters in Au(DP)/CST are very stable even under robust reaction conditions because the presence of $Au^{\delta+}$ species anchors and stabilizes Au clusters on the anionic surface of CST particles.

3.3. Temperature-Programmed Measurements and Possible Reaction Mechanisms for CO Oxidation over Au(DP)/CST. A possible reaction mechanism for CO oxidation over the Au(DP)/CST catalyst is described. For the CO oxidation at 22 °C, the TOF of 0.30 wt % Au(DP)/CST (0.027 s^{-1}) was highly similar to that of 1.0 wt % Au(DP)/CST (0.032 s^{-1}). Therefore, the catalyst with a lower Au content was applied to evaluate the Arrhenius plot for CO oxidation in the temperature range of −14 to 69 °C based on the first-order reaction rate constant k_r at each temperature (Figure S5). In this estimation, the TOF was equivalent to k_r. The E_a for CO oxidation was 19 kJ mol^{-1} at low temperatures of −14 to 22 °C, whereas it was 7.3 kJ mol^{-1} at high temperatures of 31−69 °C. Thus, the reaction mechanisms for CO oxidation differ at low and high temperatures.

CO oxidation on TiO_2-supported Au catalysts proceeds predominantly via a Au-assisted Mars−van Krevelen mechanism using lattice oxygen at reaction temperatures of 80 °C and above.[36] In this study, the contribution of lattice oxygen in CST was investigated by performing a CO reaction into CO_2 over Au(DP)/CST under He flow without O_2 by ramping the temperature from −100 to 150 °C (Figure 6a and Figure S6a,b). A peak of m/z = 44 corresponding to CO_2 was not observed from −100 to 20 °C; however, CO_2 was detected at temperatures higher than 20 °C. In Na^+−CST without Au loading (Figure 6b and Figure S6c,d), no CO_2 peaks were observed at all temperatures. Hence, the lattice oxygens of CST close to the perimeter of the Au species are used for CO oxidation at temperatures above 20 °C. In contrast, a sufficient amount of CO_2 was catalytically formed in the lower temperature range (Figure 5a). Nevertheless, CO_2 was not detected under the reaction without O_2 (Figure 6a). The O_2 species adsorbed on the CST surface close to the perimeter of the Au species, rather than lattice oxygen, were considered to contribute to CO oxidation.

Here, a possible reaction mechanism for CO oxidation over Au(DP)/CST in the low-temperature region is discussed (Figure S7). This mechanism is based on the Langmuir−Hinshelwood model and is in good agreement with the results of previous studies on other Au-loaded catalysts.[15,37−41] First, CO is reversibly adsorbed on the surface of the Au species, and part of the adsorbed CO moves to the Au perimeter on the CST surface. Subsequently, an O_2 molecule adsorbed on the perimeter is activated to produce reactive oxygen species (O*), which react with the closest CO molecule at the Au perimeter. Finally, the CO_2 is formed. The rate-determining step is considered to be the O_2 activation, as proven by the high O_2 reaction order of 0.82, whereas that of CO was 0.18 in the detailed catalytic reactions at 20 °C using 1.0 wt % Au(DP)/CST (detailed information in Figure S8).

Focusing on the reaction mechanism at high temperatures over Au(DP)/CST, CO oxidation evidently progressed according to the Mars−van Krevelen mechanism,[36] as illustrated in Figure 7. In the first CO oxidation without O_2, CO_2 was detected at 20 °C and above (Figure 6a and Figure S6a). After the spent catalyst was treated under an O_2/Ar flow at 250 °C and then cooled to −100 °C, the second CO oxidation yielded a significant amount of CO_2 at 20 °C and above (Figure S6b). This behavior confirms that the lattice oxygen atoms of the CST close to the Au perimeter were consumed for CO oxidation to form oxygen vacancies. Further, during the O_2/Ar treatment, the oxygen vacancies reacted with O_2 to regenerate lattice oxygens. Finally, the regenerated lattice oxygens repeatedly affect the CO oxidation. In addition, the lattice oxygens of the Au(DP)/CST catalyst function for CO oxidation at lower temperatures of 20 °C, compared to those of Au/TiO_2 at ∼80 °C.

4. CONCLUSIONS

Na^+−CST crystals with a sitinakite structure were prepared by hydrothermal synthesis and used as anionic supports for the Au catalysts. Au species was supported on Na^+−CST by the DP method using $Au(en)_2Cl_3$ and SI method using thiolate-protected Au colloids (∼3 nm) to obtain Au(DP)/CST and Au(SI)/CST catalysts, respectively. The TEM and XPS results indicated that 1.0 wt % Au(DP)/CST contained single Au atoms and clusters with a particle size of 1 nm or less, whereas Au(SI)/CST had only Au^0 NPs with an average particle size of

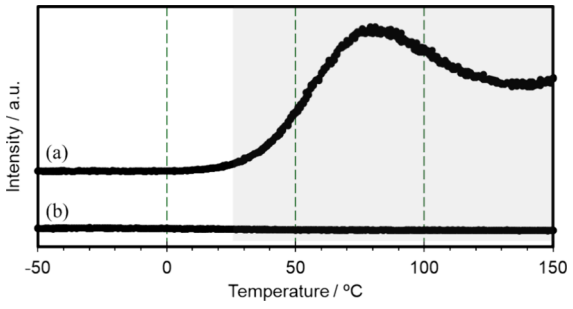

Figure 6. Temperature-programmed CO oxidation without gaseous O_2 over (a) 1.0 wt % Au(DP)/CST and (b) Na^+−CST.

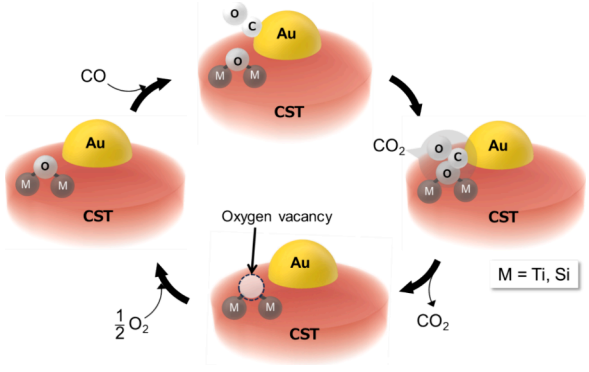

Figure 7. Possible reaction scheme for CO oxidation over the Au(DP)/CST catalyst at 20 °C and above based on the Au-assisted Mars−van Krevelen mechanism.

https://doi.org/10.1021/acsomega.4c05778
ACS Omega 2024, 9, 41696−41702

3 nm. Au(DP)/CST exhibited sufficient catalytic activity for CO oxidation even at −100 °C, and its T_{50} was −13 °C. Meanwhile, Au(SI)/CST had a high T_{50} of 38 °C. The excellent catalytic activity of Au(DP)/CST can be ascribed to extremely small Au clusters sufficiently dispersed on the CST surface for the catalytic active sites for CO oxidation at lower temperatures.

The E_a for CO oxidation over the Au(DP)/CST catalyst were 19 kJ mol^{-1} at the temperature range of −14 to 22 °C and 7.3 kJ mol^{-1} at the temperature range of 31−69 °C. This suggests that the reaction mechanism may change at a reaction temperature of approximately 20 °C. For the CO reaction into CO_2 over Au(DP)/CST under He flow without O_2, the lattice oxygens of CST close to the perimeter of the Au clusters promoted CO oxidation at temperatures above 20 °C based on the Au-assisted Mars−van Krevelen mechanism. In lower temperature regions of −80 to 20 °C, O_2 molecules adsorbed on the CST surface contributed to CO oxidation due to the well-known Langmuir−Hinshelwood mechanism. In detailed catalytic reactions at 20 °C using Au(DP)/CST, the reaction order of O_2 was approximately 1.1, whereas that of CO was 0.18. These results suggest that CO molecules were adsorbed in a near-saturated state with an O_2 activation as the rate-determining step, similar to the behavior of Au catalysts on other supports. We believe that our findings can contribute to the design of highly dispersed single-atom or cluster catalysts using the anionic surface of microporous silicotitanates and related materials with a cationic metal complex.

■ ASSOCIATED CONTENT

Supporting Information

The Supporting Information is available free of charge at https://pubs.acs.org/doi/10.1021/acsomega.4c05778.

Figure S1. High-resolution SEM images and a nitrogen adsorption isotherm of Na^+−CST. Figure S2. TEM images and the distributions of Au particle size of the pristine 1.0 wt % Au(DP)/CST, the pristine 1.0 wt % Au(SI)/CST, and the spent 1.0 wt % Au(DP)/CST. Figure S3. High magnification TEM images for the spent 1.0 wt % Au(DP)/CST catalyst. Figure S4. Au $4f_{5/2}$ and Au $4f_{7/2}$ spectra of XPS for the pristine 1.0 wt % Au(DP)/CST and the spent 1.0 wt % Au(DP)/CST. Figure S5. Activation energies of CO oxidation over 0.30 wt % Au(DP)/CST. Figure S6. Temperature-programmed CO oxidation without O_2 over 1.0 wt % Au(DP)/CST and Na^+−CST. Figure S7. Possible reaction scheme for CO oxidation over the Au/CST catalyst at 20 °C and below based on the Langmuir−Hinshelwood mechanism. Figure S8. Reaction orders of CO and O_2 in CO oxidation over 1.0 wt % Au(DP)/CST at 20 °C (PDF)

■ AUTHOR INFORMATION

Corresponding Author

Satoshi Inagaki − *Division of Materials Science and Chemical Engineering, Yokohama National University, Yokohama 240-8501, Japan;* orcid.org/0000-0002-3183-4513; Email: inagaki-satoshi-zr@ynu.ac.jp

Authors

Miyu Muraoka − *Division of Materials Science and Chemical Engineering, Yokohama National University, Yokohama 240-8501, Japan*

Takuto Miyatani − *Division of Materials Science and Chemical Engineering, Yokohama National University, Yokohama 240-8501, Japan*

Akihiro Sembuku − *Division of Materials Science and Chemical Engineering, Yokohama National University, Yokohama 240-8501, Japan*

Tamao Ishida − *Department of Applied Chemistry for Environment, Graduate School of Urban Environmental Sciences, Tokyo Metropolitan University, Hachioji, Tokyo 192-0397, Japan;* orcid.org/0000-0003-3288-1298

Toru Murayama − *Institute for Catalysis, Hokkaido University, Sapporo, Hokkaido 001-0021, Japan;* orcid.org/0000-0001-5105-3290

Yoshihiro Kubota − *Division of Materials Science and Chemical Engineering, Yokohama National University, Yokohama 240-8501, Japan;* orcid.org/0000-0001-7495-9984

Complete contact information is available at: https://pubs.acs.org/10.1021/acsomega.4c05778

Notes

The authors declare no competing financial interest.

■ ACKNOWLEDGMENTS

This work was partially supported by JSPS KAKENHI (grant numbers 22H00282 and 23K26456) and the Joint Usage/Research Center for Catalysis. STEM measurements were supported by "Advanced Research Infrastructure for Materials and Nanotechnology in Japan (ARIM)" of the Ministry of Education, Culture, Sports, Science and Technology (MEXT) (PMXP1223HK0124; Hokkaido University). This paper was supported in part by the Joint Usage/Research Center for Catalysis. The authors thank Dr. Akira Endo and Dr. Yoshihiro Kamimura (National Institute of Advanced Industrial Science and Technology) for their technical cooperation in the FE-SEM observations.

■ ABBREVIATIONS

CP, coprecipitation; CST, crystalline silicotitanate; DP, deposition−precipitation; E_a, activation energy; NP, nanoparticle; O*, reactive oxygen species; SI, sol immobilization; T_{50}, temperature for 50% CO conversion; TOF, turnover frequency; XRD, X-ray diffraction; XPS, X-ray photoelectron spectroscopy

■ REFERENCES

(1) Poojary, D. M.; Cahill, R. A.; Clearfield, A. Synthesis, Crystal Structures, and Ion-Exchange Properties of a Novel Porous Titanosilicate. *Chem. Mater.* **1994**, *6*, 2364−2368.

(2) Thorogood, G. J.; Kennedy, B. J.; Griffith, C. S.; Elcombe, M. M.; Avdeev, M.; Hanna, J. V.; Thorogood, S. K.; Luca, V. Structure and Phase Transformations in the Titanosilicate Sitinakite. The Importance of Water. *Chem. Mater.* **2010**, *22*, 4222−4231.

(3) Celestian, A. J.; Kubicki, J. D.; Hanson, J.; Clearfield, A.; Parise, J. B. The Mechanism Responsible for Extraordinary Cs Ion Selectivity in Crystalline Silicotitanate. *J. Am. Chem. Soc.* **2008**, *130*, 11689−11694.

(4) Oleksiienko, O.; Wolkersdorfer, C.; Sillanpää, M. Titanosilicates in Cation Adsorption and Cation Exchange − A Review. *Chem. Eng. J.* **2017**, *317*, 570−585.
(5) Mochizuki, C.; Inomata, Y.; Yasumura, S.; Lin, M.; Taketoshi, A.; Honma, T.; Sakaguchi, N.; Haruta, M.; Shimizu, K.; Ishida, T.; Murayama, T. Defective NiO as a Stabilizer for Au Single-Atom Catalysts. *ACS Catal.* **2022**, *12*, 6149−6158.
(6) Duan, S.; Wang, R.; Liu, J. Stability Investigation of a High Number Density Pt_1/Fe_2O_3 Single-Atom Catalyst under Different Gas Environments by HAADF-STEM. *Nanotechnology* **2018**, *29*, No. 204002.
(7) Wang, Q.; Huang, X.; Zhao, Z. L.; Wang, M.; Xiang, B.; Li, J.; Feng, Z.; Xu, H.; Gu, M. Ultrahigh-Loading of Ir Single Atoms on NiO Matrix to Dramatically Enhance Oxygen Evolution Reaction. *J. Am. Chem. Soc.* **2020**, *142*, 7425−7433.
(8) Lou, Y.; Cai, Y.; Hu, W.; Wang, Li; Dai, Q.; Zhan, W.; Guo, Y.; Hu, P.; Cao, X.-M.; Liu, J.; Guo, Y. Identification of Active Area as Active Center for CO Oxidation over Single Au Atom Catalyst. *ACS Catal.* **2020**, *10*, 6094−6101.
(9) Medvedev, D. G.; Tripathi, A.; Clearfield, A.; Celestian, A. J.; Parise, J. B.; Hanson, J. Crystallization of Sodium Titanium Silicate with Sitinakite Topology: Evolution from the Sodium Nonatitanate Phase. *Chem. Mater.* **2004**, *16*, 3659−3666.
(10) Haruta, M.; Kobayashi, T.; Sano, H.; Yamada, N. Novel Gold Catalysts for the Oxidation of Carbon Monoxide at a Temperature Far below 0 °C. *Chem. Lett.* **1987**, *16*, 405−408.
(11) Haruta, M.; Yamada, N.; Kobayashi, T.; Iijima, S. Gold Catalysts Prepared by Coprecipitation for Low-Temperature Oxidation of Hydrogen and of Carbon Monoxide. *J. Catal.* **1989**, *115*, 301−309.
(12) Hutchings, G. J. Vapor Phase Hydrochlorination of Acetylene: Correlation of Catalytic Activity of Supported Metal Chloride Catalysts. *J. Catal.* **1985**, *96*, 292−295.
(13) Nkosi, B.; Coville, N. J.; Hutchings, G. J. Vapour Phase Hydrochlorination of Acetylene with Group VIII and IB Metal Chloride Catalysts. *Appl. Catal.* **1988**, *43*, 33−39.
(14) Freund, H. J.; Meijer, G.; Scheffler, M.; Schlögl, R.; Wolf, M. CO Oxidation as a Prototypical Reaction for Heterogeneous Processes. *Angew. Chem., Int. Ed.* **2011**, *50*, 10064−10094.
(15) Haruta, M. Size- and Support-Dependency in the Catalysis of Gold. *Catal. Today* **1997**, *36*, 153−166.
(16) Taketoshi, A.; Haruta, M. Size- and Structure-Specificity in Catalysis by Gold Clusters. *Chem. Lett.* **2014**, *43*, 380−387.
(17) Okumura, M.; Fujitani, T.; Huang, J.; Ishida, T. A Career in Catalysis: Masatake Haruta. *ACS Catal.* **2015**, *5*, 4699−4707.
(18) Fujita, T.; Horikawa, M.; Takei, T.; Murayama, T.; Haruta, M. Correlation between Catalytic Activity of Supported Gold Catalysts for Carbon Monoxide Oxidation and Metal−Oxygen Binding Energy of the Support Metal Oxides. *Chin. J. Catal.* **2016**, *37*, 1651−1655.
(19) Ishida, T.; Murayama, T.; Taketoshi, A.; Haruta, M. Importance of Size and Contact Structure of Gold Nanoparticles for the Genesis of Unique Catalytic Processes. *Chem. Rev.* **2020**, *120*, 464−525.
(20) Haruta, M.; Tsubota, S.; Kobayashi, T.; Kageyama, H.; Genet, M. J.; Delmon, B. Low-Temperature Oxidation of CO over Gold Supported on TiO_2, α-Fe_2O_3, and Co_3O_4. *J. Catal.* **1993**, *144*, 175−192.
(21) Wolf, A.; Schüth, F. A Systematic Study of the Synthesis Conditions for the Preparation of Highly Active Gold Catalysts. *Appl. Catal., A* **2002**, *226*, 1−13.
(22) MOREAU, F.; BOND, G.; TAYLOR, A. Gold on Titania Catalysts for the Oxidation of Carbon Monoxide: Control of pH during Preparation with Various Gold Contents. *J. Catal.* **2005**, *231*, 105−114.
(23) Lin, M.; Mochizuki, C.; An, B.; Inomata, Y.; Ishida, T.; Haruta, M.; Murayama, T. Elucidation of Active Sites of Gold Nanoparticles on Acidic Ta_2O_5 Supports for CO Oxidation. *ACS Catal.* **2020**, *10*, 9328−9335.
(24) Lin, M.; Mochizuki, C.; An, B.; Honma, T.; Haruta, M.; Ishida, T.; Murayama, T. Ligand effect of gold colloid in the preparation of Au/Nb_2O_5 for CO oxidation. *J. Catal.* **2020**, *389*, 9−18.
(25) Murayama, T.; Ueda, W.; Haruta, M. Deposition of Gold Nanoparticles on Niobium Pentoxide with Different Crystal Structures for Room-Temperature Carbon Monoxide Oxidation. *ChemCatChem.* **2016**, *8*, 2620−2624.
(26) Zhu, H.; Liang, C.; Yan, W.; Overbury, S. H.; Dai, S. Preparation of Highly Active Silica-Supported au Catalysts for CO Oxidation by a Solution-Based Technique. *J. Phys. Chem. B* **2006**, *110*, 10842−10848.
(27) Zanella, R.; Sandoval, A.; Santiago, P.; Basiuk, V. A.; Saniger, J. M. New Preparation Method of Gold Nanoparticles on SiO_2. *J. Phys. Chem. B* **2006**, *110*, 8559−8565.
(28) Zhu, H.; Ma, Z.; Clark, J. C.; Pan, Z.; Overbury, S. H.; Dai, S. Low-temperature CO oxidation on Au/fumed SiO_2-based catalysts prepared from $Au(en)_2Cl_3$ precursor. *Appl. Catal., A* **2007**, *326*, 89−99.
(29) Zanella, R.; Delannoy, L.; Louis, C. Mechanism of Deposition of Gold Precursors onto TiO_2 during the Preparation by Cation Adsorption and Deposition−Precipitation with NaOH and Urea. *Appl. Catal., A* **2005**, *291*, 62−72.
(30) Zanella, R.; Giorgio, S.; Henry, C. R.; Louis, C. Alternative Methods for the Preparation of Gold Nanoparticles Supported on TiO_2. *J. Phys. Chem. B* **2002**, *106*, 7634−7642.
(31) Ishida, T.; Nagaoka, M.; Akita, T.; Haruta, M. Deposition of Gold Clusters on Porous Coordination Polymers by Solid Grinding and Their Catalytic Activity in Aerobic Oxidation of Alcohols. *Chem. - Eur. J.* **2008**, *14*, 8456−8460.
(32) Ishida, T.; Kinoshita, N.; Okatsu, H.; Akita, T.; Takei, T.; Haruta, M. Influence of the Support and the Size of Gold Clusters on Catalytic Activity for Glucose Oxidation. *Angew. Chem., Int. Ed.* **2008**, *47*, 9265−9268.
(33) Murayama, H.; Hasegawa, T.; Yamamoto, Y.; Tone, M.; Kimura, M.; Ishida, T.; Honma, T.; Okumura, M.; Isogai, A.; Fujii, T.; Tokunaga, M. Chloride-free and Water-soluble Au Complex for Preparation of Supported Small Nanoparticles by Impregnation Method. *J. Catal.* **2017**, *353*, 74−80.
(34) Zwijnenburg, A.; Goossens, A.; Sloof, W. G.; Crajé, M. W. J.; van der Kraan, A. M.; Jos de Jongh, L.; Makkee, M.; Moulijn, J. A. XPS and Mössbauer Characterization of Au/TiO_2 Propene Epoxidation Catalysts. *J. Phys. Chem. B* **2002**, *106*, 9853−9862.
(35) Sylvestre, J. P.; Poulin, S.; Kabashin, A. V.; Sacher, E.; Meunier, M.; Luong, J. H. T. Surface Chemistry of Gold Nanoparticles Produced by Laser Ablation in Aqueous Media. *J. Phys. Chem. B* **2004**, *108*, 16864−16869.
(36) Schlexer, P.; Widmann, D.; Behm, R. J.; Pacchioni, G. Oxidation on a Au/TiO_2 Nanoparticle Catalyst via the Au-Assisted Mars-van Krevelen Mechanism. *ACS Catal.* **2018**, *8*, 6513−6525.
(37) Ishida, T.; Koga, H.; Okumura, M.; Haruta, M. Advances in Gold Catalysts and Understanding the Catalytic Mechanism. *Chem. Rec.* **2016**, *16*, 2278−2293.
(38) Haruta, M. When Gold Is Not Notable; Catalysis by Nanoparticles. *Chem. Rec.* **2003**, *3*, 75−87.
(39) Fujitani, T.; Nakamura, I. Mechanism and Active Sites of the Oxidation of CO Over Au/TiO_2. *Angew. Chem., Int. Ed.* **2011**, *50*, 10144−10147.
(40) Remediakis, I. N.; Lopez, N.; Nørskov, J. K. CO Oxidation on Rutile-Supported Au Nanoparticles. *Angew. Chem., Int. Ed.* **2005**, *44*, 1824−1826.
(41) Laursen, S.; Linic, S. Geometric and Electronic Characteristics of Active Sites onTiO_2-Supported Au Nano-Particles: Insights from First Principles. *Phys. Chem. Chem. Phys.* **2009**, *11*, 11006−11012.

https://doi.org/10.1021/acsomega.4c05778
ACS Omega 2024, 9, 41696−41702